A newly identified pathology of episodic angioedema with hypereosinophilia (Gleich syndrome) revealed by nultiomics analysis

Tatsuya Koreeda, MS,[a] Hirokazu Muraoka, MD, PhD, MPH,[b] and Yasunori Sato, PhD[c] *Hyogo and Tokyo, Japan*

Background: Episodic angioedema with eosinophilia (Gleich syndrome) is a rare disease marked by periodic angioedema, fever, and severe eosinophilia, with limited understanding of its pathogenesis.
Objective: We sought to identify pathogenic factors contributing to severe Gleich syndrome through a comprehensive multiomics approach, using whole-genome sequencing (WGS) and RNA sequencing (RNA-seq).
Methods: A multiomics analysis was conducted on a 16- to 20-year-old female patient with severe Gleich syndrome, presenting with periodic high fever, extensive urticaria/eczema, and marked eosinophilia. The analysis included WGS and RNA-seq of blood samples.
Results: WGS revealed high-impact pathogenic mutations that have the potential to significantly alter gene function in 16 genes, including PR domain containing 16 (gene involved in transcriptional regulation). RNA-seq identified differentially expressed genes linked to immune response regulation and viral defense. Combined *z*-score analysis of WGS and RNA-seq highlighted angiotensin-converting enzyme as a key gene, with significant downregulation during disease progression that normalized with treatment. IFNG was also implicated.
Conclusions: The findings suggest that decreased angiotensin-converting enzyme expression, driven by PR domain containing 16 (gene involved in transcriptional regulation) mutations and altered IFNG expression, may contribute to increased bradykinin levels and activation of the arachidonic acid cascade, leading to the severe inflammation and angioedema characteristic of Gleich syndrome. This study underscores the utility of integrating WGS and RNA-seq data in elucidating the molecular basis of rare diseases and offers a foundation for developing therapeutic strategies for hypereosinophilic syndromes. (J Allergy Clin Immunol Global 2025;4:100465.)

Key words: *Eosinophilia, Gleich syndrome, hypereosinophilic syndrome, episodic angioedema with eosinophilia, whole-genome sequencing, RNA sequencing, multiomics analysis*

Abbreviations used

ACE:	Angiotensin-converting enzyme
DEG:	Differentially expressed gene
GO:	Gene ontology
HE:	Hypereosinophilia
HES:	Hypereosinophilic syndrome
KEGG:	Kyoto Encyclopedia of Genes and Genomes
PPI:	Protein-protein interaction
PRDM16:	PR domain containing 16 (gene involved in transcriptional regulation)
RNA-seq:	RNA sequencing
WGS:	Whole-genome sequencing

"Eosinophilia" is defined as a condition characterized by an absolute eosinophil count in the peripheral blood exceeding 500 cells/μL.[1,2] Hypereosinophilia (HE) is defined as (1) an absolute eosinophil count in the peripheral blood exceeding 1500 cells/μL in 2 blood samples taken at least 4 weeks apart; and/or (2) evidence of HE in tissues, which includes 1 or more of the following criteria: (a) eosinophils constituting more than 20% of the total nucleated cells in the bone marrow; (b) an abnormally intense eosinophilic infiltration in tissues as assessed by a pathologist; or (c) extensive deposition of eosinophil granule proteins identified by special staining techniques.[3] Hypereosinophilic syndrome (HES) is defined by the following criteria: (1) the criteria for HE are met, (2) there is organ damage caused by peripheral tissue HE, and (3) other conditions that could cause organ damage have been excluded.[3] Another syndrome associated with HE is angioedema with eosinophilia, also known as Gleich syndrome. This rare clinical entity was first described by Gerald Gleich in 1984 and is characterized by angioedema with marked eosinophilia, accompanied by fever, periodic weight gain, and urticaria.[4] HES was first proposed as a disease concept by Hardy and Anderson in 1968, with diagnostic criteria later developed by Chusid et al in 1975. Initially, it was considered a syndrome encompassing many conditions diagnosed primarily by exclusion. Since then, the causes of some conditions previously classified as HES have been clarified,[5,6] but many remain unexplained. The same applies to HE, including Gleich syndrome. The low prevalence of HE and HES, combined with the need to initiate treatment before confirming strict diagnostic criteria, has left many aspects of these diseases medically unexplored.

In recent years, genomic analysis technologies, including whole-genome sequencing (WGS), whole-exome sequencing, and targeted sequencing, have gained attention as research tools for elucidating the causes and mechanisms of diseases.[7] By comprehensively analyzing the entire spectrum of genetic variation, this technology can identify etiological genes and associated

From [a]Ikawadani-cho, Kobe-shi, Hyogo, [b]the CLINIC FOR Tamachi, Shibaura, Minato-ku, Tokyo, and [c]the Department of Preventive Medicine and Public Health, School of Medicine, Keio University, Tokyo.

Received for publication November 6, 2024; revised January 16, 2025; accepted for publication February 1, 2025.
Available online March 26, 2025.

Corresponding author: Hirokazu Muraoka, MD, PhD, MPH, CLINIC FOR Tamachi, Nagisa Terrace 4F, 3-1-32 Shibaura, Minato-ku, Tokyo 108-0023, Japan. E-mail: hirokazu_muraoka@clinicfor.life.

The CrossMark symbol notifies online readers when updates have been made to the article such as errata or minor corrections

2772-8293

https://doi.org/10.1016/j.jacig.2025.100465

factors that are challenging to detect using conventional methods. WGS is particularly effective in the study of rare diseases, where many pathologies are strongly influenced by genetic factors.[8-10] In HE and HES, somatic mutations in hematopoietic cells have been investigated using targeted sequencing, as well as the relationship between clonal proliferation of eosinophils and novel disease-related mutations, using whole-exome sequencing.[11,12] However, knowledge about the genetic background and mechanisms underlying the pathogenesis of HE and HES remains incompletely understood because few cases have been analyzed using WGS. The aim of this study was to identify pathological factors in a patient diagnosed with HE/Gleich syndrome of unknown etiology. We investigated the pathological factors of idiopathic hypereosinophilia by analyzing WGS and RNA-sequencing (RNA-seq) data obtained from this patient.

METHODS

The materials and methods are described in this article's Methods section in the Online Repository at www.jaci-global.org.

RESULTS

Clinical findings

A 19-year-old woman experienced periodic episodes of fever and myalgia, with temperatures ranging from 38°C to 40°C, accompanied by chills and shivering, occurring 1 or 2 times a month since April 2022. Around October of the same year, she developed edema, urticaria, and a generalized skin rash that left pigmentation. Blood tests from this period revealed markedly increased eosinophilia. During febrile episodes, the patient exhibited transient neutrophil predominance and significantly elevated C-reactive protein levels. Thorough examinations were conducted at the CLINIC FOR Tamachi and Gunma University Hospital. A repeated clinical examination revealed a total white blood cell count of 19,200/μL, with an eosinophil count of 16.4% (3148/μL). Hemoglobin and platelet counts were within normal limits.

Total IgE level was elevated at 504 IU/mL, but specific IgE levels for common grass and tree pollens, mites, animal dander, molds, and foods were within normal limits or negative. The patient, having been exposed to formalin, underwent a skin test for formalin sensitivity, the result for which was negative. Screening for parasitic antibodies was also negative as listed in Table E5 (in the Online Repository available at www.jaci-global.org).

Rheumatoid factor, anti–nuclear antibodies, anti–ARS antibodies, myeloperoxidase-antineutrophil cytoplasmic antibodies, PR3-ANCA, IgG, IgA, IgM, C3, C4, and total hemolytic complement were all within normal limits. A peripheral blood smear examination revealed no morphological abnormalities. Lymphocyte surface marker tests showed the following: CD7 at 56.9%, CD3 at 44.7%, CD2 at 59.3%, CD4(−)CD8(+) at 9.3%, CD4(−)CD8(−) at 48.8%, CD4(+)CD8(−) at 41.2%, CD4(+)CD8(+) at 0.7%, and a CD4/CD8 ratio of 4.19.

Various imaging studies, including computed tomography and magnetic resonance imaging, did not reveal any tumorous lesions. However, imaging showed enlarged axillary lymph nodes, splenomegaly, myositis centered around both shoulders, and bilateral pleural effusions. The soluble IL-2 receptor level was elevated at 1668 U/mL, but the pathology of the enlarged lymph nodes indicated dermatopathic lymphadenopathy, without evidence of lymphoma or malignancy, including immunostaining results. Pathological examination of the skin tissue raised a suspicion of vasculitis, though this was not definitive.

Genetic testing was performed to exclude familial Mediterranean fever and hematolymphoid neoplasms, including chronic eosinophilic leukemia. Results were negative for the FIP1L1-PDGFRα fusion gene, PDGFB split signal, FGFR1 split signal, and MEFV gene mutation, with no clonal gene rearrangement detected in the T-cell receptor beta chain Cβ1. A summary of the clinical and laboratory information is provided below (Table I), and full test results are available in this article's Online Repository at www.jaci-global.org (Supplementary Information 2).

On the basis of these results and the exclusion of autoimmune and hematological disorders and secondary eosinophilia, the patient was diagnosed with episodic angioedema with hypereosinophilia (Gleich syndrome). Treatment was initiated in July 2023 with oral glucocorticoids (prednisolone 30 mg/d), with subsequent tapering scheduled to the current maintenance dose of 1 mg/d. The patient achieved clinical and biological remission, generally by 30 days after treatment initiation and almost complete remission by 90 days.

WGS-based identification of patient-specific genetic variants and associated mutations

Patient-specific genetic variants were analyzed using WGS for diagnostic purposes. Three variant analysis tools—AnnotSV, SNPnexus, and wANNOVAR—were used. The AnnotSV analysis was filtered to include only those variants that were classified with The American College of Medical Genetics and Genomics (ACMG) class of 3 or higher (Table II). As a result, 26 variants with an ACMG class of 3 were identified, with no variants classified as more severe. Further filtering using a LOEUF_bin score of 0 identified deletion mutations in the FOXO1, PR domain containing 16 (gene involved in transcriptional regulation) (PRDM16), SPAST, ITSN1, and DLGAP2 genes. Mutations in the FOXO1 gene have been previously associated with rhabdomyosarcoma, a type of cancer. Variants in the PRDM16 gene have been linked to various cancers. Mutations in the SPAST gene are known to cause neurological disorders, particularly hereditary spastic paraplegia. However, no disease associations were identified for mutations in the ITSN1 and DLGAP2 genes.

In the SNPnexus-based analysis, the genes were listed as pathogenic according to ClinVar annotations (Table III). The analysis identified the following relevant mutations and corresponding genes: PTPRJ (rs1566734), SLC4A1 (rs121912749), FGFR4 (rs351855), and C1GALT1C1 (rs17261572). In PTPRJ, a nonsynonymous single nucleotide variant (SNV) (A/C) was found at position 44,260,501 on chromosome 17, causing an amino acid change from Q276P and associated with carcinoma of the colon. In SLC4A1, a nonsynonymous SNV (G/A) was observed in the intron region at position 177,093,242 on chromosome 5, resulting in an amino acid change to G388R, suggesting an association with cancer progression and tumor cell proliferation. A nonsynonymous SNV (A/T) was identified in C1GALT1C1 at position 120,626,774 on the X chromosome, causing an amino acid change to D131E, and was associated with polyagglutinable erythrocyte syndrome.

In wANNOVAR, we identified a series of mutations across diverse genes, focusing on exonic regions (Table IV). As a result, we detected 2 distinct frameshift mutations across multiple exons (14, 16, and 17) in the APC gene. These mutations were identified as c.5400delT (p.N1800Kfs45), c.5454delT (p.N1818Kfs45), c.5399_5400del (p.N1800Kfs7), and c.5453_5454del

TABLE I. Characteristics of the studied patient

Clinical parameter	Patient's data	Normal range
Sex	Female	—
Age of onset (y)	16-20	—
Age at diagnosis (y)	20	—
Symptoms	Angioedema	—
	Urticaria	
	Pruritus	
	Periodic fever	
	Skin rash that leaves hyperpigmentation	
	Muscle pain	
	Splenomegaly	
	Lymphadenopathy	
Serum total IgM (mg/dL)	136	46-260
Serum total IgG (mg/dL)	1384	870-1700
Serum total IgA (mg/dL)	106	110-410
Serum total IgE (IU/mL)	504	≤170
Aberrant T-cell population	No	—
C-reactive protein (mg/dL)	17.2	≤0.14
sIL-2R (U/mL)	1668	157-474
Antinuclear antibody (titer)	<1:40	<1:40
MPO-ANCA (U/mL)	<1.0	<3.5
PR3-ANCA (U/mL)	<1.0	<3.5
C3 (mg/dL)	114	86-160
C4 (mg/dL)	22	17-45
Anti–ARS antibodies (index)	<5.0	<25
EBV DNA	Not detected	—
Trunk/maxillofacial CT	Splenomegaly	—
	Enlarged axillary lymph nodes	
Trunk/maxillofacial MRI	Suspected myositis around both shoulders	—
	Reactive swelling of cervical and submandibular lymph nodes	
	Small amount of pleural effusion	
Left axillary lymph node biopsy	Findings suggestive of dermatopathic lymphadenopathy	—
	No lymphoma or malignant findings	
Skin biopsy	Possible vasculitis (unclear)	—
FIP1L1-PDGFRα fusion gene	Negative	—
PDGFB split signal	Negative	—
FGFR1 split signal	Negative	—
MEFV gene mutations	Negative	—

ARS, Aminoacyl-tRNA synthetase; *CT*, computed tomography; *MPO-ANCA*, myeloperoxidase-antineutrophil cytoplasmic antibodies; *MRI*, magnetic resonance imaging; *PR3*, proteinase 3; *sIL-2R*, soluble IL-2 receptor.

(p.N1818Kfs7), all of which were heterozygous. In OR13C8, a c.242delT mutation in exon 1 (p.A83Pfs6) was observed in a homozygous form, and in PCDH17, a c.237_238del mutation (p.D80Qfs78) was found in exon 1, also in a homozygous form. For GSPT1, multiple frameshift mutations were identified in exon 15, including c.1902_1909del (p.K635Sfs63), c.1491_1498del (p.K498Sfs63), and c.1905_1912del (p.K636Sfs*63), all of which were homozygous. In MED1, 2 heterozygous frameshift mutations were identified in exon 17, c.3210delA (p.T1071Qfs2) and c.3210_3211del (p.T1071Sfs28). In SLC35G4, synonymous SNVs c.C570T and c.C570C were detected in exon 1, both heterozygous, indicating no change in the amino acid sequence of the protein (p.G190G). In exon 4 of MADCAM1, a nonsynonymous SNV, c.T718C (p.S240P), was identified in a heterozygous form.

Enrichment analysis and protein-protein interaction network analysis using RNA-seq differentially expressed genes

The differentially expressed genes (DEGs) identified from the RNA-seq data in healthy subjects and the patient were further analyzed using gene ontology (GO) and Kyoto Encyclopedia of Genes and Genomes (KEGG) pathway analyses. Upregulated genes were significantly enriched in the biological process categories of "regulation of response to biotic stimulus" and "response to virus," as well as in the molecular function categories of "DNA-binding transcription factor binding" and "carbohydrate binding." These genes were also significantly enriched in the cellular component categories of "endocytic vesicle" and "specific granule" (Fig 1, *A*). Conversely, downregulated genes were significantly enriched in the biological process categories of "leukocyte-mediated immunity" and "cell killing," in the molecular function categories of "carbohydrate binding" and "immune receptor activity," and in the cellular component categories of "external side of plasma membrane" and "endoplasmic reticulum lumen" (Fig 1, *B*). In addition, KEGG pathway analysis revealed that the most significantly enriched gene pathways were those associated with the "PI3K-Akt signaling pathway" and "human papillomavirus infection" (Fig 1, *C*).

Next, a protein-protein interaction (PPI) network analysis was performed using the DEGs. In the PPI network, which consisted of 185 DEGs, 214 nodes and 676 edges were mapped on the basis

TABLE II. Analysis of SVs using AnnotSV

Gene	Chr	Range	Loc	MOI	GenCC_disease	OMIM_phenotype
FOXO1	13	40661542-40661624	CDS		—	Alveolar rhabdomyosarcoma
PRDM16	1	3299300-3299421	CDS	AD	Dilated cardiomyopathy, familial isolated dilated cardiomyopathy, left ventricular noncompaction, left ventricular noncompaction 8	Dilated cardiomyopathy, left ventricular noncompaction 8
PRDM16	1	3325997-3326054	CDS	AD	Dilated cardiomyopathy, familial isolated dilated cardiomyopathy, left ventricular noncompaction, left ventricular noncompaction 8	Dilated cardiomyopathy Left ventricular noncompaction 8
SPAST	2	32111248-32111315	CDS	AD;AR	Charlevoix-Saguenay spastic ataxia, hereditary spastic paraplegia 4	Spastic paraplegia 4
ITSN1	21	33876194-33876246	CDS		—	—
DLGAP2	8	999891-999994	UTR	AD	Complex neurodevelopmental disorder	—

Chr, Chromosome; *Loc*, location; *CDS*, coding sequence; *UTR*, untranslated region; *MOI*, mode of inheritance; *AD*, autosomal dominant; *AR*, autosomal reccesive; *FOXO*, forkhead box O; *SPAST*, Spastin; *ITSN*, intersectin; *DLGAP*, DLG associated protein.

TABLE III. Analysis of SNVs using SNPnexus

Gene	Chr	Region	Position	SNV	AA change	ClinVar
PTPRJ	11	Coding	48123823	A/C	Q276P	Carcinoma of colon
SLC4A1	17	Coding	44260501	C/T	G130R	Spherocytosis type 4
FGFR4	5	Intronic	177093242	G/A	G388R	Cancer progression and tumor cell motility
C1GALT1C1	X	Coding	120626774	A/T	D131E	Polyagglutinable erythrocyte syndrome

AA, Amino acid.

TABLE IV. Analysis of SNVs using wANNOVAR

Chr	Position	Exon	SNV	Gene	Exonic Func	Zygosity	HGVS
chr5	112176745	Exon 14, exon 16, exon 17	T/-	APC	Frameshift deletion	het	c.5400delT(p.N1800Kfs*45), c.5399_5400del(p.N1800Kfs*7), c.5454delT(p.N1818Kfs*45), c.5453_5454del(p.N1818Kfs*7)
chr9	107331690	Exon 1	A/-	OR13C8	Frameshift deletion	hom	c.242delT(p.A83Pfs*6)
chr13	58206917	Exon 1	T/-	PCDH17	Frameshift deletion	hom	c.237_238del(p.D80Qfs*78)
chr16	11966978	Exon 15	A/-	GSPT1	Frameshift deletion	hom	c.1902_1909del(p.K635Sfs*63), c.1491_1498del(p.K498Sfs*63), c.1905_1912del(p.K636Sfs*63)
chr17	37565264	Exon 17	A/-	MED1	Frameshift deletion	het	c.3210delA(p.T1071Qfs*2), c.3210_3211del(p.T1071Sfs*28)
chr18	11610164	Exon 1	G/T	SLC35G4	Synonymous SNV	het	c.C570T(p.G190G)
chr18	11610164	Exon 1	G/C	SLC35G4	Synonymous SNV	het	c.C570C(p.G190G)
chr19	501719	Exon 4	T/C	MADCAM1	Nonsynonymous SNV	het	c.T718C(p.S240P)

HGVS, Human Genome Variation Society.

of protein-protein interactions, with interaction scores greater than 0.7 (Fig 1, *D*). Using an interaction score greater than 0.95 to identify hub genes, the most highly connected hub genes were RSAD2 (degree = 9), MX1 (degree = 8), ISG15 (degree = 8), and IFI44L (degree = 7). A heatmap of the DEGs and a volcano plot showing the time-series changes in each gene expression level are provided in Fig E2 (in the Online Repository available at www.jaci-global.org).

Identification of key genes using *Z*-score analysis

Variants from WGS data labeled as HIGH in annotation impact, along with gene expression levels from RNA-seq data and centrality scores from PPI network analysis, were evaluated using *z*-score analysis (Table V). Among the *Z* scores, IFI27 had the highest value (*Z* score: 4.47619923). OAS2 (degree: 19) and angiotensin-converting enzyme (ACE) (ABS_log2FC: 9.10262032) exhibited the highest centrality score and absolute $\log_2$ fold change, respectively. The smallest adjusted *P* value was observed for IFI27 (P_{adj}: 4.18×10^{-65}). The effects of the mutations were as follows: splice acceptor variant and intron variant in 3 cases, start lost and conservative inframe deletion in 1 case, frameshift variant in 3 cases, stop lost in 1 case, stop gained in 2 cases, and splice donor variant and intron variant in 1 case. *Z*-score values were used for GO term and KEGG pathway enrichment analysis as well as PPI network analysis (see Fig E3 in

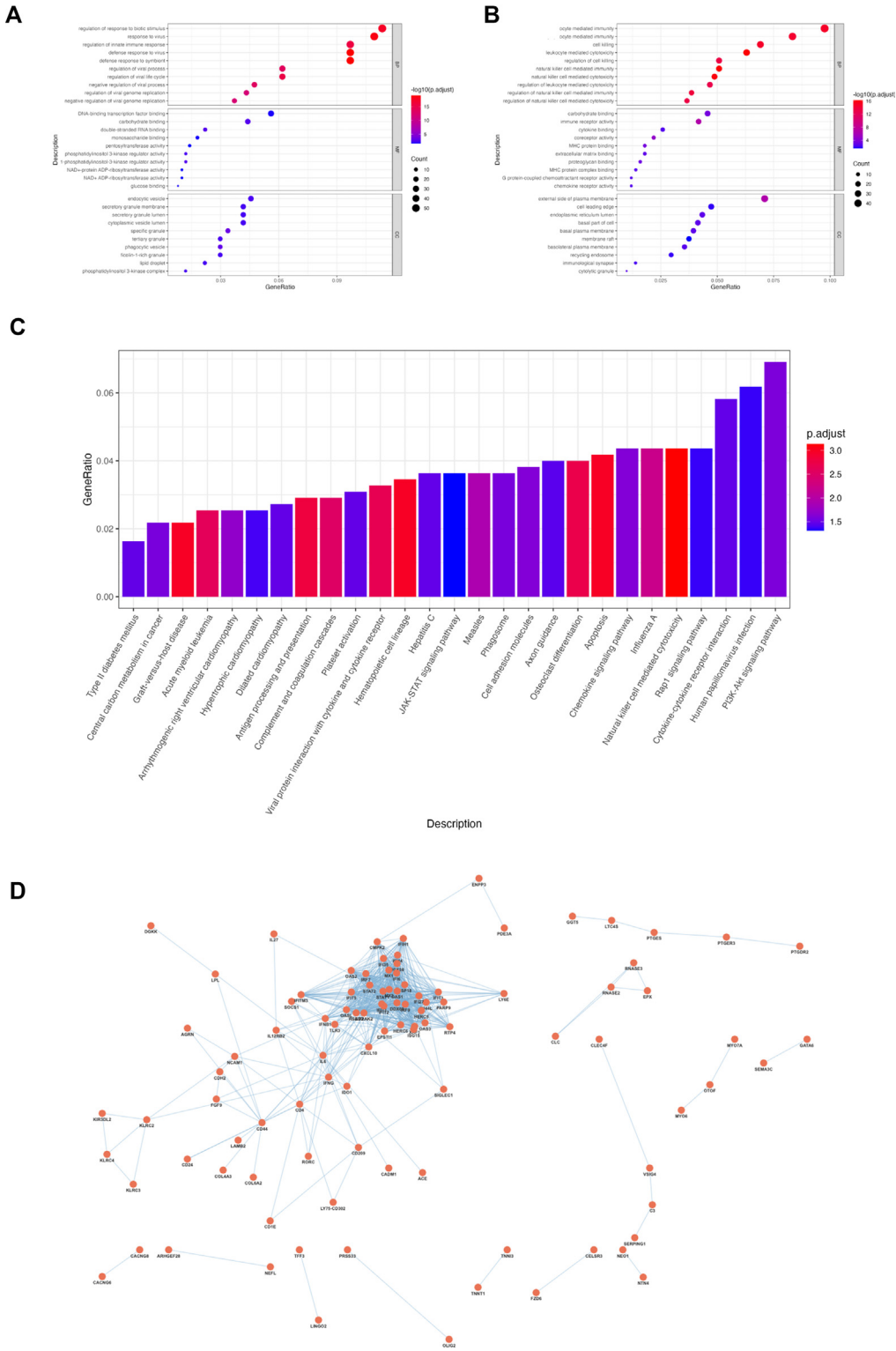

FIG 1. Pathway enrichment analysis using GO and KEGG, and PPI network analysis. Pathway enrichment analysis using GO and KEGG terms, and PPI network analysis based on patient RNA-seq data. (**A**) Pathway enrichment analysis using GO terms for DEGs of patient-derived upregulated genes in biological process (BP), molecular function (MF), and cellular component (CC) categories. The top 10 terms in each category are shown. (**B**) Pathway enrichment analysis using GO terms for DEGs of patient-derived downregulated genes. (**C**) Pathway enrichment analysis using KEGG terms for DEGs of patient-derived genes with variable expression. (**D**) Pathway enrichment analysis using GO terms for DEGs of patient-derived genes with variable expression. The vertical axis represents the percentage of DEGs in each term. PPI network analysis using DEGs of patient-derived genes with variable expression. Red circles represent nodes, and blue lines represent edges.

TABLE V. Identification of key disease-associated genes based on *Z*-score values

Gene	POS	Variant	Effect	Degree	ABS_log$_2$FC	P_{adj}	Z_score
IFI27	14:94105764	G/T	splice_acceptor_variant & intron_variant	14	7.22991464	4.18×10^{-65}	4.47619973
IFI27	14:94115784	TGGCCATGGC/T	start_lost & conservative_inframe_deletion	14	7.22991464	4.18×10^{-65}	4.47619973
IFI44	1:78662885	G/GT	frameshift_variant	18	3.62858894	1.20×10^{-30}	3.63485564
OAS2	12:113010483	A/G	stop_lost	19	2.51335138	7.25×10^{-23}	3.33028482
EPSTI1	13:42888298	T/TTCAGG	frameshift_variant	17	3.22174861	6.81×10^{-18}	3.27200626
ACE	17:63486300	C/A	stop_gained	4	9.10262032	0.00107677	3.11768804
MSR1	8:16186158	C/T	splice_donor_variant & intron_variant	4	3.28217749	5.35×10^{-04}	0.73409481
COL6A2	21:46125455	A/AC	splice_acceptor_variant & intron_variant	1	3.28721175	7.06×10^{-18}	0.34946627
SIGLEC10	19:51417359	C/T	splice_acceptor_variant & intron_variant	2	1.88542826	1.09×10^{-08}	−0.0807563
RETSAT	2:85350974	TA/T	frameshift_variant	3	1.48768267	2.26×10^{-04}	−0.1410527
CC2D2A	4:15480736	C/T	stop_gained	1	1.84782388	4.07×10^{-04}	−0.4083765

ABS, Absolute value; *FC*, fold change; *POS*, position.

this article's Online Repository at www.jaci-global.org). The plots of Effect Type count values for genomic variants in this patient are provided in Fig E4 (in the Online Repository available at www.jaci-global.org).

Dynamics of gene expression in pretreatment and posttreatment time series

The temporal changes in expression levels for selected genes were assessed. For each gene group, $\log_2$ fold changes were calculated at 3 time points: pretreatment, 1 month, and 3 months posttreatment. Significant changes in expression levels were observed when comparing pretreatment samples to those from healthy subjects, particularly for the genes ACE, CC2D2A, COL6A2, EPST11, IFI27, IFI44, MSR1, OAS2, RETSAT, and SIGLEC10 (Fig 2, *A*). Overall, many genes exhibited significant temporal changes in expression levels compared with pretreatment. For example, EPST11 was strongly upregulated before treatment, with this upregulation alleviated after 1 month and further reduced after 3 months. A similar pattern was observed for IFI27, IFI44, and CC2D2A. Conversely, ACE and RETSAT exhibited a reverse trend, with marked suppression of expression before and 1 month posttreatment, followed by recovery after 3 months. PTPRJ and SIGLEC10 showed reduced expression at 1 and 3 months posttreatment compared with healthy subjects, whereas OR13C8 and SLC35G had a read count of 0 in both the patient and healthy subjects. Enrichment analysis revealed that GO terms related to the regulation of immune response, leukocyte-mediated immunity, and cell killing were enriched in pretreatment samples but were no longer enriched at 1 and 3 months posttreatment (Fig 2, *B*). In contrast, GO terms involved in chemotaxis, cell migration, and cell differentiation were newly enriched at 1 and 3 months posttreatment. The pretreatment samples were plotted in the third quadrant, whereas the 1- and 3-month posttreatment samples were plotted in the first quadrant (Fig 2, *C*). A heatmap identified genes with high loading on the negative axis of PC1, including BFAR, XG, RCE1, and COL18A1 (Fig 2, *D*). For each gene showing a recovery trend after 3 months, the OMIM database was used to search for causative genes with phenotypes similar to those observed in the patient. The results indicated that a decrease in ACE led to an increase in bradykinin, contributing to the development of angioedema.[13,14]

Exploration of upstream and master regulators of the ACE gene by Ingenuity Pathway Analysis

Analysis of the dynamics of gene expression in pretreatment and posttreatment time series suggested a relationship between the ACE gene and the patient with the disease. To further explore this, we investigated the relationship between the ACE gene and the disease by visualizing upstream regulators and causal networks using Ingenuity Pathway Analysis (IPA) for the ACE gene. When we searched for upstream regulators of ACE using pretreatment RNA-seq data, we found that the IFNG gene had the highest Activation *Z* score of 4.403 (see Fig E5, *A*, in this article's Online Repository at www.jaci-global.org). Similarly, in the causal network's Activation *Z* scores, the IFNG gene also had the highest Activation *Z* score of 4.217 (Fig E5, *B*). The network visualization showed an interaction from IFNG in the extracellular space to ACE in the plasma membrane (Fig E5, *C*). To further investigate the association between IFNG and this patient, a drill-down analysis using IPA for the IFNG gene identified an association with idiopathic eosinophilia.[6] Pathways enriched in IPA for this disease, including pathway diagrams for RNA virus infection and network diagrams for angioedema, which are suggested to be relevant to the disease pathogenesis, are provided in Figs E6 and E7 (in the Online Repository available at www.jaci-global.org).

DISCUSSION

The aim of this study was to identify the pathological factors in a patient diagnosed with HE/Gleich syndrome of unknown etiology using WGS and RNA-seq analysis.

The patient presented with clinical symptoms consistent with Gleich syndrome, including marked eosinophilia exceeding 5000/μL at its peak, periodic fever, and recurrent edema and urticaria. However, the patient also exhibited a generalized skin rash with pathological findings of vasculitis and pigmentation, transient neutrophil-predominant leukemoid reactions associated with fever, markedly elevated C-reactive protein levels, and splenomegaly. These findings are not commonly observed in

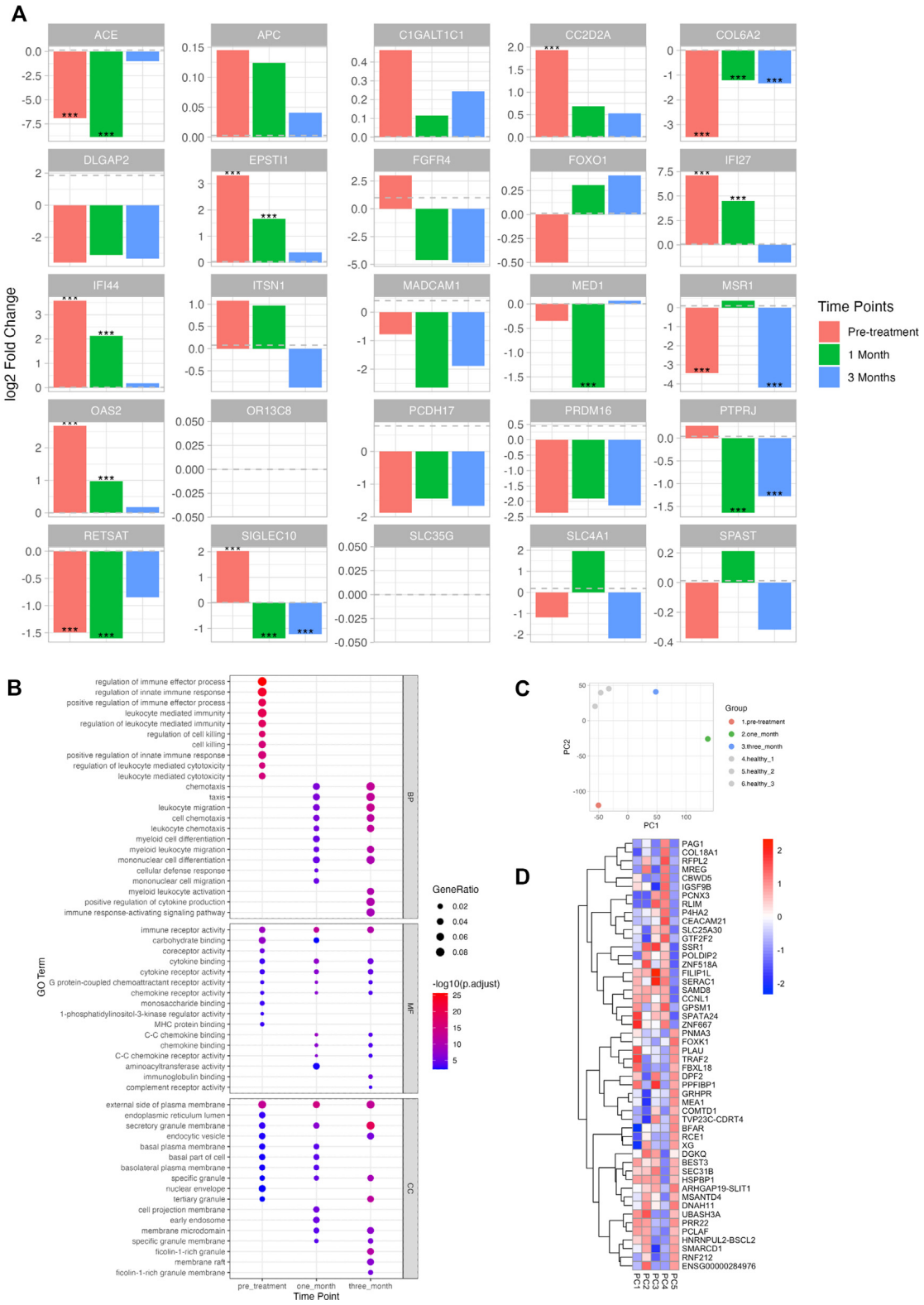

FIG 2. Analysis of time-series changes in gene expression levels and pathway enrichment. Analysis of changes in gene expression levels and enriched pathways using patient samples collected at pretreatment, 1-month, and 3-month time points. (**A**) Comparison of expression levels of candidate target genes at each time point. Three asterisks indicate an adjusted *P* value of less than .01, representing a significant difference from the healthy group. (**B**) Transition of enriched GO terms at each time point, representing biological process (BP), molecular function (MF), and cellular component (CC). (**C**) PCA plot using RNA-seq data from healthy subjects and patient at each time point. (**D**) PCA for each gene. Heatmap displaying loading values, showing PC1 to PC5, clustered in rows. *PCA*, Principal-component analysis.

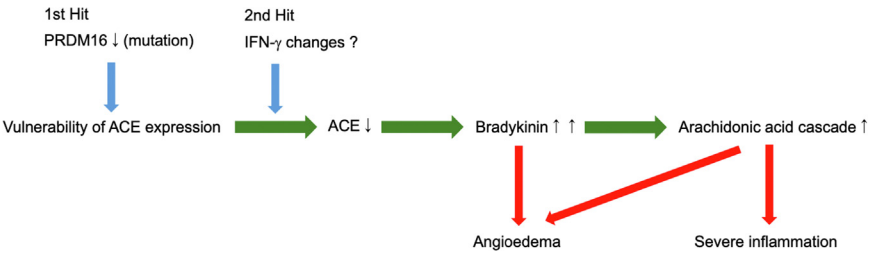

FIG 3. The role of ACE as a pathogenic factor in a type of HE/Gleich syndrome. This figure illustrates the pathway by which a PRDM16 mutation leads to pathogenic outcomes in HE/Gleich syndrome. The mutation downregulates ACE expression, resulting in elevated bradykinin levels. This triggers the arachidonic acid cascade, which contributes to both angioedema and severe inflammation. In addition, IFN-γ levels influence ACE expression, further exacerbating these processes.

Gleich syndrome, but similar cases have been reported.[15-17] Although this patient did not meet the strict diagnostic criteria for HES, because eosinophilic infiltration was not clearly demonstrated in various organ assessments, some consider Gleich syndrome itself to be a broader category of HES.[3] This reflects the fact that the disease concepts of HE and HES are not fully defined, and their classification has evolved over time. In any case, the patient exhibited a very advanced and dramatic clinical presentation, with no spontaneous remission for more than 6 months, leading to a diagnosis of severe Gleich syndrome after all other differential diagnoses were ruled out.

Gleich syndrome is a rare disease with no currently approved or clearly defined diagnostic criteria, and to date, fewer than 100 adult cases have been reported.[16] Nevertheless, patients with Gleich syndrome typically present with homogeneous clinical symptoms and well-characterized laboratory findings, suggesting that the disease should be considered a distinct eosinophilic disorder, likely caused by a common pathogenic mechanism.[17] In cases with clear and intense symptoms, as in this case, even a small number of disease samples are likely to lead to the identification of some pathological factors by multiomics analysis, which is very significant for the purpose of elucidating the pathology of rare diseases. This is very significant for the purpose of elucidating the pathology of rare diseases.

In addition, within the molecular function category, several GO terms were enriched for carbohydrate binding, monosaccharide binding, glucose binding, proteoglycan binding, and glycan-related genes, such as "pentosyltransferase activity." Glycosylation is a common posttranslational modification of proteins and lipids and serves as a critical recognition determinant in cell-immune system interactions. Immune and stromal cells are equipped with glycan-binding proteins that sense and decode diverse glycans.[18,19] This network of glycans and glycan-binding proteins is crucial for the recognition of pathogens and the regulation of inflammatory and autoimmune responses, with alterations in the cellular glycome ultimately leading to pathological phenotypes.[20-22] C1GALT1C1 (rs17261572), also known as Cosmc, identified in variant analysis, galactosylates Tn antigen (GalNAcα1-Ser/Thr-R) during the biosynthesis of mucin-type O-glycans to core 1 Galβ1-3GalNAcα1-Ser/Thr (T antigen)[23] (see Fig E8 in this article's Online Repository at www.jaci-global.org). Given that glycans function as drug recognition markers, the potential involvement of glycan-related genes in drug regulation has been investigated in public database analyses.[24] The relationship between rs17261572 on C1GALT1C1 and HE/Gleich syndrome, as well as its connection to other glycan-related genes, warrants further investigation.

The *Z*-score values derived from WGS annotation impact, along with the ranking of DEGs and PPI network analysis from RNA-seq data, identified IFI27, OAS2, and ACE as key candidate genes. In this case, the expression levels of these genes were variable compared with healthy subjects and showed a recovery trend after treatment. It is well established that a reduction in ACE leads to an increase in bradykinin, which contributes to the development of angioedema.[13,14] Bradykinin itself induces angioedema[25] and further increases phospholipase A2 activity, enhances arachidonic acid metabolism, and triggers a wide range of inflammatory responses.[26] In addition, large amounts of bradykinin have been reported to recruit eosinophils.[26,27] In this patient, who presented with severe systemic inflammation in addition to edema, ACE was found to play a major role as a pathological factor. The patient achieved a good state of remission with oral prednisolone treatment, not only due to the general anti-inflammatory effects of corticosteroids but also because corticosteroids have been suggested to directly restore ACE expression,[28] which may have contributed to the improvement in the condition.

Notably, there is a case report of a patient with congenital ACE deficiency presenting with recurrent angioedema.[29] This finding further supports the involvement of ACE as a pathological factor in diseases characterized by angioedema. However, in the present case, no mutation in the ACE gene itself critically defines a loss of expression, suggesting that an alteration in an upstream factor leading to reduced ACE expression may be involved.

PRDM16, a gene with a confirmed structural abnormality in this case, has been shown to reduce ACE mRNA expression in the systemic RAAS when conditionally knocked out in the heart, although the detailed mechanism remains unclear.[30] Although ACE expression in the intrarenal RAAS is compensated for in this conditionally knocked out model, it is plausible that the PRDM16 mutation observed in this patient results in a systemic reduction in ACE expression.

Although the direct mechanism by which PRDM16 mutations lead to reduced ACE expression is not fully understood and warrants further investigation, the 2-hit model will be proposed (Fig 3). Namely, based on the PRDM16 mutation, some acquired event that causes an INF-γ "storm" is the trigger, leading to abnormal activation of the bradykinin pathway through reduced ACE. In this case, hyperactive eosinophil biology was not observed, which is probably because eosinophilia was caused mainly by the ACE-bradykinin pathway. This may explain the difference in clinical presentation from eosinophilia caused by strictly immunologic mechanisms (ie, secretion of eosinophil-stimulating signals such as IL-5 from T_H2 and/or ICL2 cells).

This study has certain limitations. Gleich syndrome does not behave as a genetic disorder, and the pathological model is highly speculative. Although it is certainly significant that newly identified factors such as ACE and PRDM16 can be involved in the pathogenesis, these results would need to be confirmed in a larger cohort. Although multiomics analyses using WGS and RNA-seq have advanced our understanding of the pathogenesis of HE/Gleich syndrome at the genetic and gene expression levels, these approaches must be supplemented with protein-level analyses and *in vivo* model-based studies. Confirming blood levels of bradykinin and ACE would further substantiate the pathogenesis of this condition. Moreover, other factors influencing ACE expression need to be investigated, and detailed mechanisms must be elucidated. Gene expression data alone do not adequately capture posttranslational modifications, protein interactions, or functional dynamics within cells and tissues. *In vivo* models can provide a more comprehensive understanding of disease mechanisms within a physiological context. Therefore, future research should incorporate proteomic analyses, gene editing techniques, and animal models.

DISCLOSURE STATEMENT

There are no sources of funding to declare for the research reported in this manuscript.

Disclosure of potential conflict of interest: The authors declare that they have no relevant conflicts of interest.

We sincerely thank the patient and subjects who participated in this study for their invaluable cooperation. We also express our deepest appreciation to Dr Hirokazu Muraoka for his extensive guidance and support throughout the entirety of this study. His contributions spanned from the conceptualization of the research, the collection of blood samples, and the acquisition of WGS and RNA-seq data, to the writing, editing, and discussion of the manuscript. All data produced in the present study are available on reasonable request to the authors.

Key messages

- **PRDM16 mutations and decreased ACE expression likely contribute to severe inflammation and angioedema in Gleich syndrome.**
- **Integration of WGS and RNA-seq data reveals molecular insights that could aid in developing therapies for hypereosinophilic syndromes.**

REFERENCES

1. Roufosse F, Weller PF. Practical approach to the patient with hypereosinophilia. J Allergy Clin Immunol 2010;126:39-44.
2. Rothenberg ME. Eosinophilia. N Engl J Med 1998;338:1592-600.
3. Valent P, Klion AD, Horny HP, Roufosse F, Gotlib J, Weller PF, et al. Contemporary consensus proposal on criteria and classification of eosinophilic disorders and related syndromes. J Allergy Clin Immunol 2012;130:607-12.e9.
4. Gleich GJ, Schroeter AL, Marcoux JP, Sachs MI, O'Connell EJ, Kohler PF. Episodic angioedema associated with eosinophilia. Trans Assoc Am Physicians 1984;97:25-32.
5. Cools J, DeAngelo DJ, Gotlib J, Stover EH, Legare RD, Cortes J, et al. A tyrosine kinase created by fusion of the PDGFRA and FIP1L1 genes as a therapeutic target of imatinib in idiopathic hypereosinophilic syndrome. N Engl J Med 2003;348:1201-14.
6. Simon HU, Plötz SG, Dummer R, Blaser K. Abnormal clones of T cells producing interleukin-5 in idiopathic eosinophilia. N Engl J Med 1999;341:1112-20.
7. Van El CG, Cornel MC, Borry P, Hastings RJ, Fellmann F, Hodgson SV, et al. Whole-genome sequencing in health care: recommendations of the European Society of Human Genetics. Eur J Hum Genet 2013;21:580-4.
8. Ashley EA, Butte AJ, Wheeler MT, Chen R, Klein TE, Dewey FE, et al. Clinical assessment incorporating a personal genome. Lancet 2010;375:1525-35.
9. Lupski JR, Reid JG, Gonzaga-Jauregui C, Rio Deiros D, Chen DCY, Nazareth L, et al. Whole-genome sequencing in a patient with Charcot-Marie-Tooth neuropathy. N Engl J Med 2010;362:1181-91.
10. Roach JC, Glusman G, Smit AFA, Huff CD, Hubley R, Shannon PT, et al. Analysis of genetic inheritance in a family quartet by whole-genome sequencing. Science 2010;328:636-9.
11. Lee JS, Seo H, Im K, Park SN, Kim SM, Lee EK, et al. Idiopathic hypereosinophilia is clonal disorder? Clonality identified by targeted sequencing. PLoS One 2017;12:e0185602.
12. Andersen CL, Nielsen HM, Kristensen LS, Søgaard A, Vikeså J, Jønson L, et al. Whole-exome sequencing and genome-wide methylation analyses identify novel disease associated mutations and methylation patterns in idiopathic hypereosinophilic syndrome. Oncotarget 2015;6:40588-97.
13. Ghebrehiwet B, Joseph K, Kaplan AP. Complement activation in hereditary angioedema: classical and lectin pathways involvement. Front Allergy 2024;5:1302605.
14. Straka BT, Ramirez CE, Byrd JB, Stone E, Woodard-Grice A, Nian H, et al. Effect of bradykinin receptor antagonism on ACE inhibitor-associated angioedema. J Allergy Clin Immunol 2017;140:242-8.e2.
15. Basso JR, Bizinoto LGZ, Limone GA, Enokihara MMSS, Do Espirito-Santo Filho K, Fonseca AR, et al. Hereditary angioedema with normal C1 inhibitor and F12 mutations in 42 Brazilian families. Braz J Med Biol Res 2021;54.
16. Mormile I, Petraroli A, Loffredo S, Rossi FW, Mormile M, Del Mastro A, et al. Hereditary angioedema: a comprehensive review of treatment options and management of acute attacks. J Clin Med 2021;10:1442.
17. Khoury P, Herold A, Alpaugh A, Dinerman E, Holland-Thomas N, Stoddard J, et al. Episodic angioedema with eosinophilia (Gleich syndrome) is a multilineage cell cycling disorder. Haematologica 2015;100:300-7.
18. Alves I, Fernandes Â, Santos-Pereira B, Azevedo CM, Pinho SS. Glycans on the crossroad of health and disease: challenges and opportunities. FEBS Lett 2022;596:1485-502.
19. Pinho SS, Alves I, Gaifem J, Rabinovich GA. From inflammation to metastasis: glycans as dynamic regulators of macrophage heterogeneity. Cell Mol Immunol 2023;20:1101-13.
20. Ohtsubo K, Marth JD. Glycosylation in cellular mechanisms of health and disease. Cell 2006;126:855-67.
21. Pinho SS, Reis CA. Glycosylation in cancer: mechanisms and clinical implications. Nat Rev Cancer 2015;15:540-55.
22. Rabinovich GA, Croci DO. Regulatory circuits mediated by lectin-glycan interactions in autoimmunity and cancer. Immunity 2012;36:322-35.
23. Wang Y, Ju T, Ding X, Xia B, Wang W, Xia L, et al. Cosmc is an essential chaperone for correct protein O-glycosylation. Proc Natl Acad Sci U S A 2010;107:9228-33.
24. Koreeda T, Honda H. Aberrant glycosylation in autoimmune diseases: a review. Glycoconj J 2024;41:133-49.
25. Cicardi M, Zuraw BL. Angioedema due to bradykinin dysregulation. J Allergy Clin Immunol Pract 2018;6:1132-41.
26. Kaplan AP, Joseph K, Silverberg M. Pathways for bradykinin formation and inflammatory disease. J Allergy Clin Immunol 2002;109:195-209.
27. Roisman GL, Lacronique JG, Desmazes-Dufeu N, Carré C, Le Cae A, Dusser DJ. Bradykinin receptor antagonists modulate bronchial response to ultrasonically nebulized distilled water in patients with common cold. Am J Respir Crit Care Med 2012;153:381-90.
28. Fishel RS, Eisenberg S, Shai SY, Redden RA, Bernstein KE, Berk BC. Glucocorticoids induce angiotensin-converting enzyme expression in vascular smooth muscle. Hypertension 1995;25:343-9.
29. Sreeram AB, Corey JP. Glucocorticoid-induced bradykinesia. Otolaryngol Head Neck Surg 1995;112:421-3.
30. Kang JO, Ha TW, Jung HU, Lim JE, Oh B. A cardiac-null mutation of Prdm16 causes hypotension in mice with cardiac hypertrophy via increased nitric oxide synthase 1. PLoS One 2022;17:e0267938.